Cation-π interaction regulates ligand-binding affinity and signaling of integrin $\alpha_4\beta_7$

YouDong Pan[a], Kun Zhang[a], JunPeng Qi[a], Jiao Yue[a], Timothy A. Springer[b,1], and JianFeng Chen[a,1]

[a]Laboratory of Molecular Cell Biology, Institute of Biochemistry and Cell Biology, Shanghai Institutes for Biological Sciences, Chinese Academy of Sciences, Shanghai 200031, China; and [b]The Immune Disease Institute, Children's Hospital Boston, and Department of Pathology, Harvard Medical School, 3 Blackfan Circle, Boston, MA 02115

Contributed by Timothy A. Springer, October 15, 2010 (sent for review August 20, 2010)

Integrin $\alpha_4\beta_7$ mediates rolling and firm adhesion of leucocytes, two of the critical steps in leukocyte migration and tissue specific homing. Affinity of $\alpha_4\beta_7$ for ligand is dynamically regulated by three interlinked metal ion-binding sites in β_7-subunit I domain. In this study, we found that Phe185 (F185), a highly conserved aromatic residue in β_7-subunit, links the specificity-determining loop and the synergistic metal ion-binding site (SyMBS) through cation-π interaction. Mutations of F185 that disrupted the SyMBS cation-F185 interaction led to deficient firm cell adhesion mediated by high affinity $\alpha_4\beta_7$, and only slightly affected rolling adhesion mediated by low affinity $\alpha_4\beta_7$. Disruption of SyMBS cation-F185 interaction induced partial extension of integrin ectodomain and separation of cytoplasmic tails, and impaired $\alpha_4\beta_7$-mediated bidirectional signaling. In addition, loss of SyMBS cation-F185 interaction increased paxillin expression and promoted paxillin-integrin binding, leading to deficient cell spreading. Furthermore, integrin $\alpha_4\beta_7$-mediated cell migration was decreased by the abolishment of SyMBS cation-F185 interaction. Thus, these findings reveal a cation-π interaction playing vital roles in the regulation of integrin affinity, signaling, and biological functions.

Integrins are a family of α/β heterodimeric cell adhesion molecules that mediate cell-cell, cell-matrix, and cell-pathogen interactions. Different from most integrins that mediate only firm adhesion of cells upon activation, integrin $\alpha_4\beta_7$ can mediate both rolling and firm adhesion of lymphocytes on its ligand mucosal addressing cell adhesion molecule-1 (MAdCAM-1), which make it indispensable in the homing of lymphocytes to the intestine and gut-associated lymphoid tissues (1).

Cell adhesion through integrin is dependent on the dynamic regulation of integrin affinity. Affinity regulation is associated with the conformational rearrangement of the integrin molecule. Previous studies have shown that integrin extracellular domains exist in at least three distinct global conformational states: bent with a closed headpiece, extended with a closed headpiece, and extended with an open headpiece (2). The closed and open headpieces have low and high affinity for ligand, respectively. The equilibrium among these different states is regulated by integrin inside-out signaling and certain extracellular stimuli, such as divalent cations (3, 4). Compared to the low affinity state in $Ca^{2+} + Mg^{2+}$, removal of Ca^{2+} strikingly increases ligand-binding affinity and adhesiveness of integrins (5). Crystal structures of integrin $\alpha_V\beta_3$ and $\alpha_{IIb}\beta_3$ revealed a unique interlinked linear array of three divalent cation-binding sites in integrin β I domain (6, 7). The central metal ion-dependent adhesion site (MIDAS) is flanked by two metal ion-binding sites, the adjacent to MIDAS (ADMIDAS) and synergistic metal ion-binding site (SyMBS). The divalent cation at MIDAS directly coordinates the acidic side chain shared by all integrin ligands, and is essential for integrin-ligand binding (8–10). The SyMBS and ADMIDAS function as positive and negative regulatory sites, respectively (8, 9). The occupancy of SyMBS by divalent cation is required for integrin activation, whereas inhibition of integrin-ligand binding by Ca^{2+} is mediated by the ADMIDAS. Although the importance of SyMBS cation has been reported, the mechanism for its positive regulatory function has not been elucidated because hardly any conformational change was observed around the SyMBS upon integrin activation and ligand binding (6, 7).

Another important regulatory element for integrin-ligand binding is specificity-determining loop (SDL), a 20-30 residue segment located between β strands 2 and 3 in the β I domain (11). Mutations or deletion of SDL disrupted integrin-ligand binding (11, 12). Switching of a seven-residue sequence within the SDL of β_1 integrin with the homologous sequence in β_3 integrin leads to the alteration of ligand-binding specificity (13). Because SDL is a fairly flexible loop, orientation could be critical for its function. However, the mechanism of SDL orientation control remains elusive.

In this study, we found that SyMBS and SDL were linked by a cation-π interaction formed between SyMBS cation and F185 in integrin β_7 subunit and that this interaction is essential for integrin affinity regulation and signaling. Disruption of SyMBS cation-F185 interaction impaired $\alpha_4\beta_7$-MAdCAM-1 high affinity binding and induced global conformational change of $\alpha_4\beta_7$ which induced abnormal intracellular signaling.

Results

A Cation-π Interaction Is Predicted to Link the SyMBS and SDL in Integrin β Subunit I Domain. To investigate the regulatory element in integrin β_7 subunit, integrin β_3 I domain structure was chosen to serve as the structure model for the following reasons: (*i*) Integrin β I domain is highly conserved among different β subunits; for example, the sequence identities of β_7 I domain to the structurally characterized β_2 and β_3 I domain are 66% and 53%, respectively (Fig. S1*A*); (*ii*) The β I domain structure is also highly conserved because the β_3 and β_2 I domain structures are almost identical as shown from superposition of β I domains from $\alpha_{IIb}\beta_3$ and $\alpha_X\beta_2$ (Fig. S1*B*) (14, 15); (*iii*) The crystal structures of integrin $\alpha_{IIb}\beta_3$ in both open and closed conformations have the highest resolution among currently available integrin structures, and have been widely used as a model for the study of other integrins (6, 8–10, 15). Thus, the integrin β_3 I domain structure is an excellent model for β_7 I domain.

F185, located at the base of SDL and adjacent to the SyMBS cation, is conserved as Phe or Tyr in all integrin β subunits except for β_4 (Fig. 1*A*). The structure-based sequence alignment of $\alpha_{IIb}\beta_3$ and $\alpha_X\beta_2$ showed that all the residues in contact with F185 and SyMBS cation are identical among β_7, β_2, and β_3 subunits (Fig. S1*C*). Based on the crystal structure of integrin $\alpha_{IIb}\beta_3$ (liganded-open conformation, pdb 2vdl) (15), the SyMBS cation is aligned on the center of the phenyl ring and the distances between them are within the range of cation-π interaction (<6.0 Å) (16) (Fig. 1 *B–D*). Therefore, it is predicted that a

Author contributions: T.A.S. and J.C. designed research; Y.P., K.Z., J.Q., and J.Y. performed research; Y.P., K.Z., J.Q., J.Y., and J.C. analyzed data; and T.A.S. and J.C. wrote the paper.

The authors declare no conflict of interest.

[1]To whom correspondence may be addressed. E-mail: springer@idi.harvard.edu or jfchen@sibs.ac.cn.

This article contains supporting information online at www.pnas.org/lookup/suppl/doi:10.1073/pnas.1015487107/-/DCSupplemental.

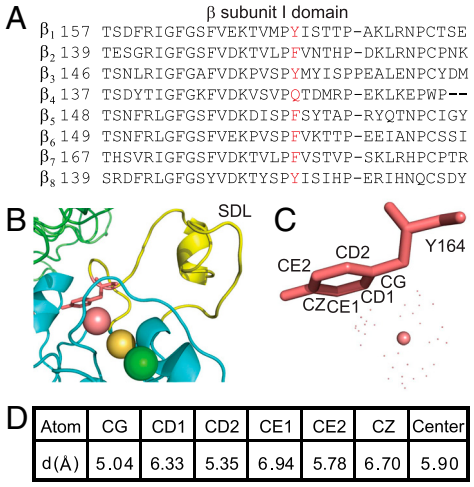

Fig. 1. Potential cation-π interaction links SDL and SyMBS in integrin β_7 subunit I domain. (*A*) Sequence alignment of the human integrin β subunit I domains. Residues at the position of F185 in β_7 are shown in red. (*B*) Detailed view of the metal ion cluster, Y164 (F185 in β_7) and SDL in integrin β_3 I domain (pdb 2vdl). SyMBS, MIDAS, and ADMIDAS metal ions are magenta, gold, and green spheres, respectively. (*C* and *D*) Distances between SyMBS cation and Y164 aromatic ring.

cation-π interaction is formed between SyMBS cation and F185. Moreover, an axis drawn through the three metal ions is aligned with the phenyl ring (Fig. 1*B*).

The Aromatic Side Chain of F185 Is Essential for Integrin High Affinity Ligand Binding. To test our hypothesis, F185 was mutated to Tyr (Y), Trp (W), His (H), or Ala (A) respectively to gradually weaken its ability of forming cation-π bond (17). Phe, Tyr, and Trp can form cation-π bonds with adjacent cations as they all have aromatic rings which are electron rich near their centers and poor around their peripheries. Phe and Tyr contribute similarly to the cation-π bond due to the identical size of their aromatic rings, whereas Trp has a substantially larger aromatic side chain and would require repacking of residues around it to form cation-π bond. Although His is also aromatic, it does not form a cation-π bond, because His has a different electrostatic distribution and the preferred site for interaction with a cation is on the edge of the ring opposite the unprotonated nitrogen atom (17). Substitution of Phe with Ala results in the complete removal of the aromatic group.

Adhesive behavior of $\alpha_4\beta_7$ 293T transient transfectants in shear flow was characterized in a parallel wall flow chamber by allowing them to adhere to MAdCAM-1 adsorbed to its lower wall. 293T cell line is used in this study because it does not express endogenous $\alpha_4\beta_7$ integrin. The shear stress was incrementally increased and the velocity of the cells remaining bound at each increment was determined. Wild-type (WT) transfectants behaved as previously described for lymphoid cells expressing $\alpha_4\beta_7$ (8). In 1 mM Ca^{2+} + 1 mM Mg^{2+}, cells rolled with increasing velocity as shear stress was increased, reaching a velocity of about 8 μm/s at the wall shear stress of 16 dyn/cm^2, and were mostly detached at 32 dyn/cm^2 (Fig. 2*A*). By contrast, cells were firmly adherent in 1 mM Mg^{2+} (Fig. 2*A*). Rolling and firm adhesion represent low and high affinity interactions of $\alpha_4\beta_7$ with MAdCAM-1, respectively. As control, cells transfected with the α_4 cDNA alone, or $\alpha_4\beta_7$ transfectants treated with the $\alpha_4\beta_7$ blocking antibody Act-1 or EDTA did not accumulate on MAdCAM-1 substrates (Fig. 2*A*).

F185 substitutions had little impact on $\alpha_4\beta_7$-mediated rolling adhesion of 293T transient transfectants in Ca^{2+} + Mg^{2+} (Fig. 2*A*). In contrast, weakening of the aromatic ring's ability to form a cation-π bond significantly affected the firmly adhesive behavior of cells in Mg^{2+} (Fig. 2 *A* and *B*). Substitution of Phe by Tyr had no impact on firm adhesion, whereas substitution of Phe by Trp converted the firm adhesion of cells in Mg^{2+} to rolling adhesion. Retention of the aromatic side chain but abolition of ability to form a cation-π bond with His substitution, or mutation to Ala abolished $\alpha_4\beta_7$-MAdCAM-1 binding in Mg^{2+} (Fig. 2 *A* and *B*). Next we tested the effect of F185 mutations on the strength of $\alpha_4\beta_7$-mediated adhesion to MAdCAM-1 by examining the cell resistance to detachment. While resistance to detachment was similar in Ca^{2+} + Mg^{2+}, in Mg^{2+} WT and F185Y were similarly resistant, and the F185W, F185H, and F185A mutants were increasingly susceptible (Fig. 2 *C* and *D*).

To further confirm that F185 is required for integrin high affinity ligand binding, we investigated the effect of F185 mutations on a highly activated $\alpha_4\beta_7$ mutant (Q324T). Q324T mutation was reported to activate integrin by introducing a N-glycan at N322 in the β I/hybrid domain interface, which induces β_7 hybrid domain swing-out (18). Consistently, F185W, F185H, and F185A mutations severely impaired the high affinity ligand binding of Q324T mutant in both ion conditions (Fig. 2*E*). Taken together, these data demonstrate that an aromatic side chain capable of forming a cation-π bond at residue 185 is essential for high affinity ligand binding.

F185 Functions Through Cation-π Interaction by Interacting with the SyMBS Cation. To exclude the possibility that, instead of cation-π interaction, F185 performs its function by forming hydrophobic or charge-charge interactions with its nearby environment, F185 was mutated to Leu (L, hydrophobic residue) and Glu (E, negatively charged residue), respectively. The adhesive behavior of F185L and F185E 293T transient transfectants on MAdCAM-1 was similar to that of F185A transfectants (Fig. 3*A*), suggesting that the contribution of F185 to $\alpha_4\beta_7$-MAdCAM-1 binding was not through hydrophobic or charge-charge interactions.

To confirm that F185 functions through its interaction with SyMBS cation, mutation abolishing cation binding at SyMBS was introduced into F185 mutants. Previous study on integrin $\alpha_4\beta_7$ has shown that mutation of SyMBS-coordinating residue D237 stabilizes integrin in the low affinity state (8). If F185 functions through interacting with SyMBS cation, removal of SyMBS cation by mutation should eliminate the effects of F185 mutations. As predicted, F185 mutation to W, H, or A had no effect in the context of the D237A mutation (Fig. 3*B*). Moreover, removal of SyMBS cation by mutation rescued the cell adhesion of F185H and F185A mutants to a level similar to that of the SyMBS single mutant, suggesting the abolishment of ligand binding by F185H and F185A mutations is dependent on SyMBS cation. These results suggest that the regulatory function of F185 is dependent on the SyMBS cation, and support a cation-π bond.

The SyMBS Cation-F185 Interaction Is Essential for Coupling Integrin-Ligand Binding and Global Conformational Change. We used FRET to examine the influence of F185 residue on integrin conformation. To assess the orientation of integrin $\alpha_4\beta_7$ ectodomain relative to the plasma membrane, $\alpha_4\beta_7$ was labeled with Alexa Fluor 488-Act-1 Fab fragment as donor which binds to the top of $\alpha_4\beta_7$ β I domain (19). The plasma membrane was labeled with FM4-64 FX (FM) as acceptor (7). Binding of MAdCAM-1 to $\alpha_4\beta_7$ did not influence Act-1 Fab binding (Fig. S2). Compared to WT, the FRET efficiency of F185A 293T transient transfectants was significantly lower when cells spread on poly-L-Lysine (PLL) (Fig. 4*A*), indicating that the ectodomain of $\alpha_4\beta_7$ F185A mutant was more extended prior to ligand binding. Binding of MAdCAM-1 to $\alpha_4\beta_7$ further decreased the FRET efficiency of both WT and F185A $\alpha_4\beta_7$ expressing cells. In MAdCAM-1 and 0.5 mM Mn^{2+}, FRET efficiency of WT and F185A transfectants was even lower, and similar (Fig. 4*A*), suggesting full extension of the $\alpha_4\beta_7$ ectodomain.

The influence of SyMBS cation-F185 interaction on integrin cytoplasmic domain separation was assessed using 293T cells transiently expressing $\alpha_4\beta_7$ with monomeric cyan fluorescent protein

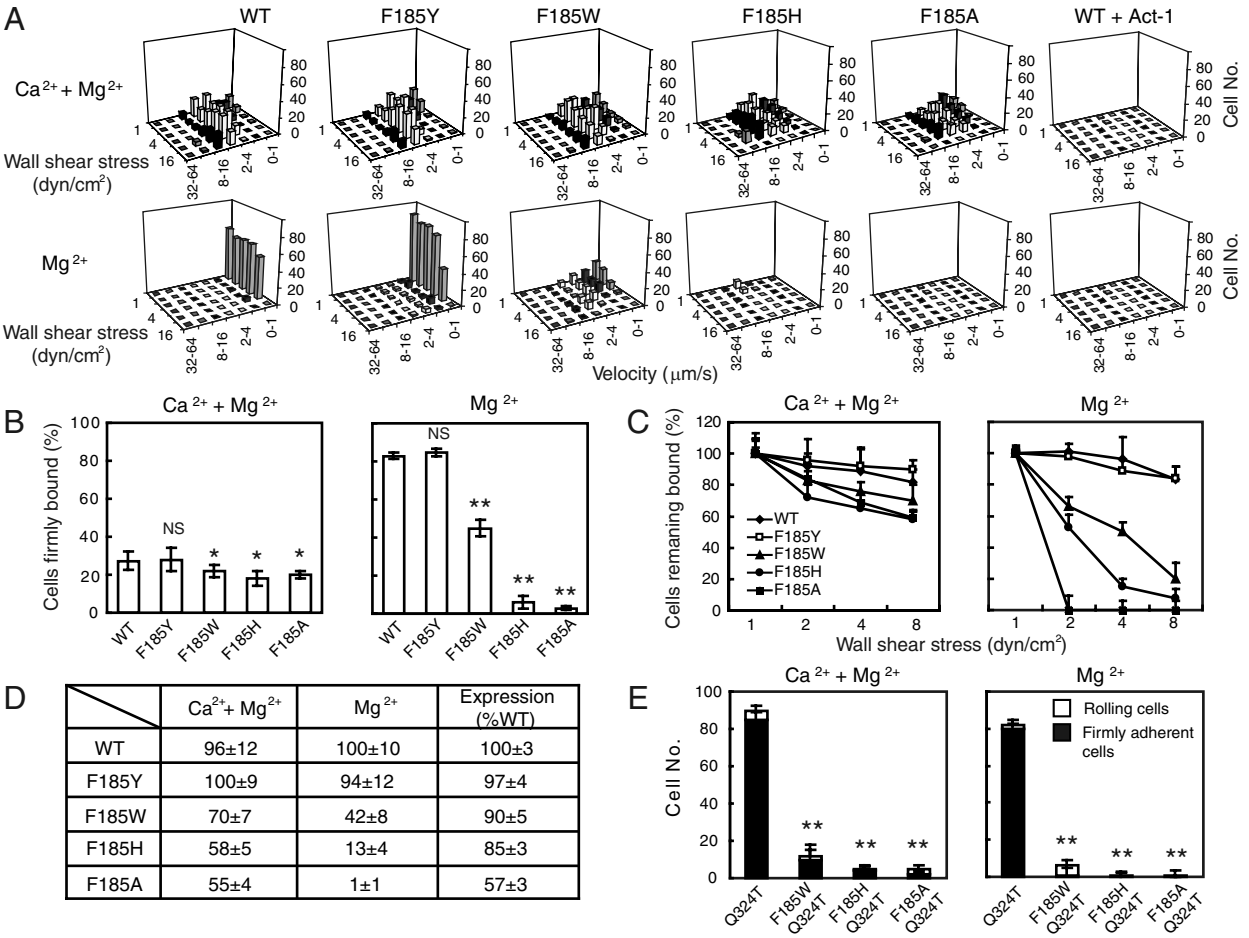

	Ca^{2+}+ Mg^{2+}	Mg^{2+}	Expression (%WT)
WT	96±12	100±10	100±3
F185Y	100±9	94±12	97±4
F185W	70±7	42±8	90±5
F185H	58±5	13±4	85±3
F185A	55±4	1±1	57±3

Fig. 2. Effect of F185 mutations on the adhesive modality of $\alpha_4\beta_7$. (*A*) Adhesive behavior of $\alpha_4\beta_7$ 293T cell transfectants on h-MAdCAM-1/Fc in shear flow. Rolling velocity was measured for all adherent cells and plotted as a distribution at each wall shear stress. (*B*) Percentage of cells firmly bound to ligand in the indicated divalent ions under the wall shear stress of 1 dyn/cm^2. (*C*) Cell resistance to detachment in shear flow. The total number of cells remaining bound at increasing wall shear stresses was determined as a percent of adherent cells at 1 dyn/cm^2. (*D*) The initial number of bound cells at 1 dyn/cm^2 and integrin cell surface expression level. (*E*) Adhesive behavior of Q324T wedge mutant and F185/Q324T double mutant $\alpha_4\beta_7$ transfectants under the wall shear stress of 1 dyn/cm^2. Error bars are ±s.d. ($n = 3$). *: $P < 0.05$; **: $P < 0.01$; and NS, not significant.

(mCFP) and yellow fluorescent protein (mYFP) fused to the C termini of α_4- and β_7- subunits respectively (20). These fusions do not affect integrin function (9, 20). F185A mutation induced partial separation of integrin cytoplasmic domains prior to and after MAdCAM-1 binding, and MAdCAM-1 plus 0.5 mM Mn^{2+} induced more separation of the $\alpha_4\beta_7$ cytoplasmic tails (Fig. 4*B*), similar to the results of the extension FRET assay in Fig. 4*A*.

SyMBS Cation-F185 Interaction Is Required for Integrin $\alpha_4\beta_7$-Mediated Inside-Out Signaling. Talin is a cytoskeletal protein that binds to integrin β tail and activates integrin by inside-out signaling (21).

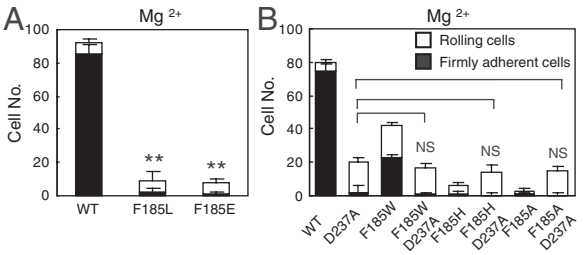

Fig. 3. F185 functions through cation-π interaction by interacting with the SyMBS cation. (*A*) Adhesive behavior of F185L and F185E 293T transfectants under the wall shear stress of 1 dyn/cm^2. (*B*) The number of rollingly or firmly adherent cells bearing WT and mutant $\alpha_4\beta_7$ was measured under the wall shear stress of 1 dyn/cm^2. Error bars are ±s.d. ($n = 3$), **: $P < 0.01$.

To investigate the impact of SyMBS cation-F185 interaction on integrin-mediated inside-out signaling, talin-GFP was overexpressed in $\alpha_4\beta_7$ 293T transient transfectants (Fig. S3*A*). In $Ca^{2+} + Mg^{2+}$, the percentage of firmly bound WT $\alpha_4\beta_7$ transfectants to total bound cells was increased from 36% to 70% after cotransfection with talin-GFP, indicating the activation of integrin by talin (Fig. 5*A*). In contrast, the percentage of firmly bound F185W mutant transfectants was not increased by cotransfection with talin-GFP (Fig. 5*A*), suggesting impaired integrin-mediated inside-out signaling. Loss of cation-π interaction did not alter the binding of endogenous talin to $\alpha_4\beta_7$ because a similar amount of talin was coimmunoprecipitated with WT and mutant $\alpha_4\beta_7$ (Fig. S3*B*). Interestingly, talin cleavage was inhibited in F185 mutant transfectants (Fig. S3*B*).

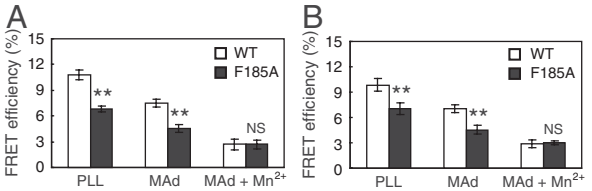

Fig. 4. Influence of F185 mutations on integrin conformation. (*A*) FRET between integrin $\alpha_4\beta_7$ β I domain and the plasma membrane. (*B*) Intersubunit FRET between integrin $\alpha_4\beta_7$ cytoplasmic domains. Error bars are ±s.d. ($n = 10$), **: $P < 0.01$.

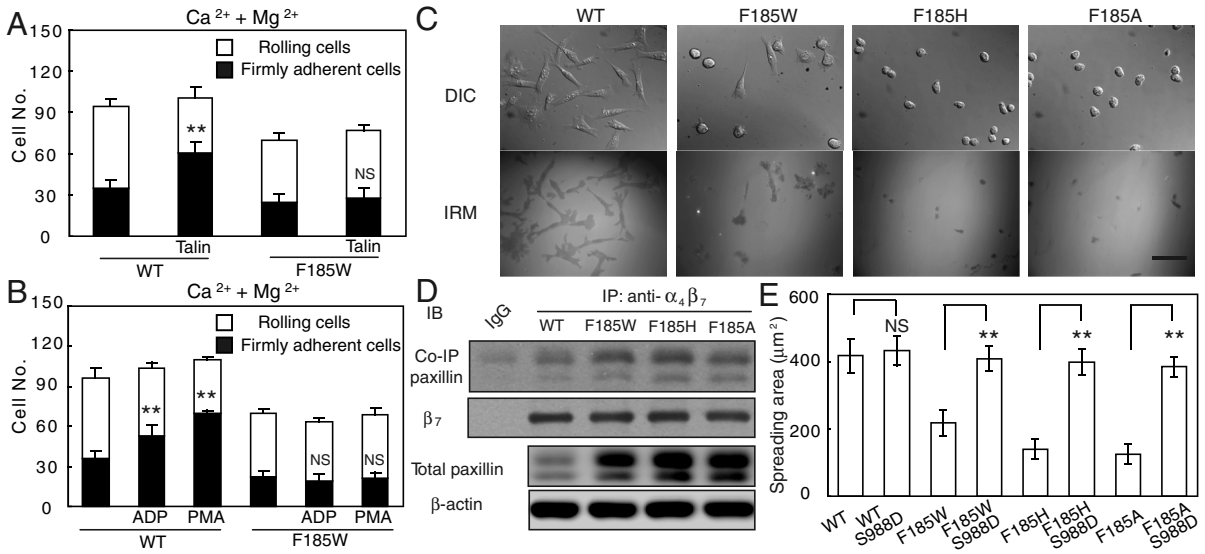

Fig. 5. Effect of F185 mutations on integrin $\alpha_4\beta_7$-mediated bidirectional signaling. (*A*) The number of rollingly and firmly adherent WT and F185W transfectants under the shear stress of 0.4 dyn/cm^2 with or without cotransfection of talin. Error bars are ±s.d. ($n = 3$). (*B*) The number of rollingly and firmly adherent WT and F185W 293T transfectants under the shear stress of 0.4 dyn/cm^2 pre or poststimulation by ADP or PMA. Error bars are ±s.d. ($n = 3$). (*C*) DIC and IRM images of $\alpha_4\beta_7$ CHO-K1 stable transfectants. The images are representatives from one of three independent experiments. Bar, 50 μm. (*D*) Coimmunoprecipitation of paxillin with integrin $\alpha_4\beta_7$. Total paxillin and β-actin are shown in the lower rows. (*E*) Quantification of cell spreading area of 293T transfectants expressing $\alpha_4\beta_7$ WT or S988D mutations. Error bars are ±s.d. ($n = 50$), **: $P < 0.01$.

To further confirm the impaired inside-out signaling, we tested integrin activation by adenosine diphosphate (ADP) or phorbol 12-myristate 13-acetate (PMA) stimuli in WT and F185W expressing 293T transient transfectants, which express ADP receptors P2Y1,2,4 (22). ADP and PMA were reported to induce integrin activation through inside-out signaling by activating phosphatidylinositol 3-kinase (PI3K) pathway (23, 24). Consistently, WT $\alpha_4\beta_7$ but not F185W transfectants could be activated by ADP or PMA (Fig. 5*B*).

Loss of SyMBS Cation-F185 Interaction Blocks Integrin $\alpha_4\beta_7$-Mediated Cell Spreading. To assess the requirement of the cation-π interaction for integrin-mediated outside-in signaling, CHO-K1 cells stably expressing similar level of WT or mutant $\alpha_4\beta_7$-GFP were established which showed similar adhesive behavior as 293T transfectants (Fig. S4 *A* and *B*), and $\alpha_4\beta_7$-mediated cell spreading was studied (Fig. 5*C*). CHO-K1 transfectants were allowed to adhere on immobilized MAdCAM-1 for 2 h in F12 medium with Ca^{2+}+ Mg^{2+}, followed by fixation and microscopic analysis. WT $\alpha_4\beta_7$ expressing cells spread substantially on MAdCAM-1 substrates. Interference-reflection microscopy (IRM) showed an irregular shape and extensive area of cell-substrate contact (Fig. 5*C*). In contrast, the F185W stable transfectants exhibited less spreading. F185H and F185A transfectants did not spread on MAdCAM-1; the area of contact with MAdCAM-1 was much smaller and largely remained round (Fig. 5*C*). Quantification of cell area from differential interference contrast (DIC) images showed F185H and F185A transfectants exhibited the same area of projection as cells in suspension (Fig. S4*C*). Moreover, these cells failed to form significant actin stress fibers in contrast to the robust stress fibers in WT transfectants (Fig. S4*D*). Thus, F185 mutation abrogates $\alpha_4\beta_7$-mediated cell spreading, suggesting disrupted outside-in signaling.

Loss of SyMBS Cation-F185 Interaction Enhances Association of Integrin with Paxillin. To address the question of how the loss of cation-π interaction affects integrin-mediated cell spreading, the association of integrin with paxillin was examined. Paxillin is a focal adhesion-associated adaptor protein important in the regulation of cell spreading and migration (25, 26). Compared to WT $\alpha_4\beta_7$ CHO-K1 stable transfectants, paxillin expression was up-regulated and more paxillin was coimmunoprecipitated with $\alpha_4\beta_7$ in F185 mutant transfectants (Fig. 5*D*). Quantitative real-time PCR and immunoblot analysis demonstrated that the up-regulation of paxillin occurs at the transcription level in mutant transfectants (Fig. S5).

To confirm that the impaired cell spreading is due to enhanced paxillin-integrin binding, a point mutation (S988D) was introduced into integrin α_4 subunit cytoplasmic domain that inhibits association with paxillin (26). As expected, S988D mutation restored the spreading of F185 mutant CHO-K1 stable transfectants to the same level as that of WT $\alpha_4\beta_7$ expressing cells (Fig. 5*E* and Fig. S6*A*). The recovery was not due to the alteration of $\alpha_4\beta_7$-MAdCAM-1 binding because the adhesive behavior of $\alpha_4\beta_7$ expressing cells was not affected by S988D mutation (Fig. S6*B*). These findings demonstrate that loss of SyMBS cation-F185 interaction up-regulates paxillin expression, enhances the association of integrin with paxillin, and thus, results in deficient cell spreading.

Abolishment of SyMBS Cation-F185 Interaction Impairs $\alpha_4\beta_7$ Integrin-Mediated Cell Migration. Integrin-mediated cell adhesion and signaling play a fundamental role in cell migration (27). We investigated the role of SyMBS cation-F185 interaction on $\alpha_4\beta_7$-mediated cell migration using $\alpha_4\beta_7$ CHO-K1 stable transfectants. In contrast to 75% wound closure of WT $\alpha_4\beta_7$ expressing cells, cells expressing F185A mutant showed only 19% wound closure after migrating on MAdCAM-1 for 9 h (Fig. 6*A*; Movies S1 and S2). Random cell migration of F185A transfectants was also reduced significantly with shorter migration traces compared to WT (Fig. 6*B*, Movies S3 and S4). The F185A expressing cells exhibited elongated cell shape and detachment at the trailing edge was retarded (Movies S3 and S4). Similar results were obtained from serum-induced transwell migration. Compared to WT, the number of F185A transfectants migrating to the lower chamber was decreased significantly (Fig. 6*C*). Thus, these results demonstrate that mutation of F185 impairs $\alpha_4\beta_7$-mediated cell migration.

Discussion

The dynamic regulation of integrin affinity and signaling plays vital roles in cell spreading and migration. As metalloproteins, ligand binding of integrins is dependent on and regulated by divalent cations. Although previous studies have shown the importance of the SyMBS cation, the mechanism for its positive regulatory

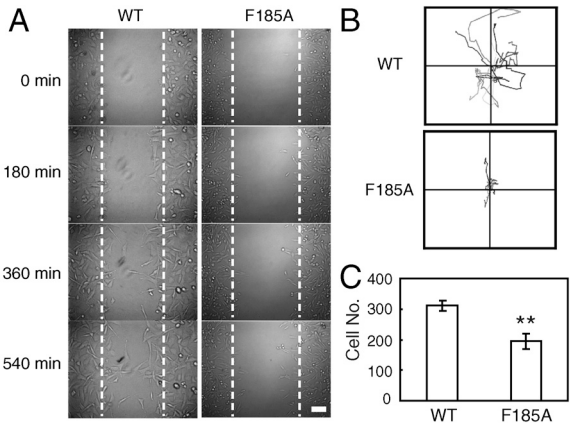

Fig. 6. Effect of F185 mutations on integrin $\alpha_4\beta_7$-mediated cell migration. (*A*) Wound-healing migration of CHO-K1 stable cells. Representative images are from Movies S1 and S2 at the indicated time. Bar, 50 μm. (*B*) Single cell random migration of CHO-K1 stable cells. Migration tracks of ten randomly picked cells are shown. (*C*) Serum-induced transwell migration. Cells migrating to the lower chamber were counted. Error bars are ±s.d. ($n = 3$), **: $P < 0.01$.

function remains elusive. On the other hand, SDL is a fairly flexible loop which is important for integrin-ligand binding, but how its orientation is controlled has not been elucidated. In this study, we revealed that a cation-π interaction links the SyMBS cation with F185 in the SDL and regulates $\alpha_4\beta_7$ ligand binding and signaling.

The residue at the position of F185 in integrin β_7 I domain is conserved as Phe or Tyr in all integrin β subunits except for β_4, which is unusual in many respects. Different from other integrins that harbor short cytoplasmic domains of 40–70 amino acids, β_4 contains a cytoplasmic domain of 1,088 amino acids, and interacts with intermediate filaments rather than the actin cytoskeleton (28). Hence, integrin β_4 could have distinct mechanisms for affinity and signaling regulation.

Upon activation, integrin undergoes global and local conformational rearrangements to convert from a low affinity to high affinity state (2). The lack of SyMBS cation-F185 impairs high affinity adhesion and appears to disrupt the local conformational change of ligand-binding site required for high affinity integrin-ligand binding. Interestingly, mutations of SyMBS-coordinating residues also impaired integrin high affinity ligand binding (8), suggesting that this cation-π interaction may exert its role in stabilizing the high affinity state of integrins by modulating the electronic environment of the metal ions in the ligand-binding site. In addition, it is worthwhile to note that F185 locates at the base of SDL, which is a fairly flexible loop near the metal ion-binding sites. Therefore, the metal ions might regulate the conformation of SDL during integrin activation through this cation-π interaction.

Despite deficient activation of ligand binding by F185 mutations, loss of SyMBS cation-F185 interaction induces partial extension of integrin ectodomain and separation of cytoplasmic tails which are associated with integrin activation (Fig. 4 *A* and *B*). Previous structural and mutagenesis studies have shown the importance of the α1-helix, β6-α7 loop, and α7-helix in allosteric communication between the β I and hybrid domains (29–31). In the high affinity, liganded integrin conformation, the α1-helix straightens and moves laterally, displacing the β6-α7 loop and facilitating the downward displacement of the α7-helix that triggers hybrid domain swing-out and global conformational rearrangements (29). The interlinked SyMBS, MIDAS, and ADMIDAS comprise residues in the α1-helix and β6-α7 loop. Breaking SyMBS cation-F185 interaction could affect the interlinked metal ions cluster, and then induce the above conformational rearrangements. However, ligand binding can be dissociated from these rearrangements except those close to the ligand-binding site (9, 32). Our results suggest that F185 mutations prevent shift of MIDAS toward the high affinity configuration and, at the same time, release structural constraints on the β6-α7 loop and α7-helix that trigger global conformations similar to those in the high affinity state.

Another notable finding of our study is that the loss of cation-π interaction up-regulates paxillin expression at transcriptional level. Paxillin is a 68-kDa intracellular signaling adaptor protein that is involved in cellular responses to integrin-dependent adhesion and migration. Previous study has shown that paxillin expression can be up-regulated at the transcription level through growth factor receptor (GFR) activation, such as HER2/HER3 (33). As a common consequence of GFR activation, the activity of some tyrosine kinases, such as PI-3-kinase (PI3K) and mitogen-activated protein kinase (MAPK), is increased, leading to phosphorylation and activation of transcription factors (34, 35). In our study, we have shown that F185 mutations induce partial extension of $\alpha_4\beta_7$ and separation of its cytoplasmic tails, which are associated with integrin activation (20). These conformational changes might mimic integrin outside-in signaling and activate similar intracellular pathways in response to integrin activation, such as increase of PI3K and MAPK activity (36, 37).

Paxillin binding to the cytoplasmic domain of α_4 integrins results in inhibition of cell spreading (25). Consistent with the decreased cell spreading, paxillin-$\alpha_4\beta_7$ binding is increased in F185 mutant transfectants. The overexpression of paxillin can increase the paxillin binding to WT $\alpha_4\beta_7$ and inhibit cell spreading (Fig. S6 *C–E*), suggesting the increase in paxillin expression alone is sufficient to increase paxillin binding to $\alpha_4\beta_7$ and decrease cell spreading independent of F185 mutations. Thus, it is more likely that the increased binding of paxillin to F185 mutants is due to the increased paxillin protein level, but not the higher affinity of $\alpha_4\beta_7$ mutant to paxillin.

Integrin-mediated cell migration requires the dynamic regulation of cell adhesion at the leading edge and de-adhesion at the trailing edge with the cooperation of multiple signaling pathways (38). Up-regulation of integrin adhesiveness in integrin $\alpha_4\beta_7$ led to the elongation of cell shape, deficiency of cell retraction at the trailing edge, and inhibition of cell migration (39). Interestingly, down-regulation of integrin adhesiveness by F185 mutations resulted in a similar phenotype in our study (Fig. 6*B*, Movies S3 and S4). Therefore, integrin requires both low and high affinity ligand binding to support optimal cell migration. Besides the deficient cell adhesion, the loss of SyMBS cation-π interaction could generate defective intracellular signaling which up-regulates paxillin expression and leads to constitutively enhanced association of paxillin with $\alpha_4\beta_7$. The effective cell migration requires the dynamic spatial regulation of α_4 integrin-paxillin binding at the cell leading and trailing edges (26, 40). Either disrupting or enforcing the association of α_4 with paxillin greatly impairs cell migration. Thus, the enhanced α_4-paxillin association by F185 mutations could result in deficient cell migration. In addition, talin cleavage is decreased by F185 mutations which could slow focal adhesion (FA) turnover and lead to accumulation of mature FA (41). As expected, more mature FAs were observed in migrating F185 mutant expressing cells than in WT transfectants (Fig. S7), which could also contribute to the decreased cell migration.

Materials and Methods

cDNA Construction. The β_7 site-directed mutations were generated by using Quick-change (Stratagene). cDNA of human talin with N-terminal-fused green fluorescent protein (talin-GFP) in vector pEGFP-C1 was kindly provided by Minsoo Kim (University of Rochester Medical Center, USA). All constructs were confirmed by DNA sequencing.

Flow Chamber Assay. The flow chamber assay was performed as described (8). For the experiments of ADP and PMA stimulation, 10 μM ADP or 0.1 μM PMA (final concentration) were added and incubated at 37 °C for 10 min before cells were infused into the flow chamber.

FRET. FRET was measured as described (7, 20). For detecting the orientation of integrin ectodomain relative to cell membrane, cells were incubated on

indicated ligands for 30 min at 37 °C. 0.5 mM Mn^{2+} was added into medium to activate integrin. Adherent cells were fixed by 3.7% paraformaldehyde and then stained with 20 μg/mL Alexa Fluor 488-Act-1 Fab, followed by staining with 10 μM FM-4-64 FX (Invitrogen). For detecting the association of integrin cytoplasmic tails, α_4-mCFP/β_7-mYFP293T transient transfectants (10^6/mL) were treated as above and allowed to incubate at 37 °C for 2 h. Then cells were fixed and subjected to photobleach FRET imaging. FRET efficiency (E) was calculated as $E = 1\text{-}(FCFP(d)_{Pre}/FCFP(d)_{Post})$, where $FCFP(d)_{Pre}$ and $FCFP(d)_{Post}$ are the mean CFP emission intensity of Pre- and Post- photobleaching.

Cell Spreading and Microscopy. Cell spreading was done as described (42). Cells were allowed to spread on human MAdCAM-1 fused to the Fc1, 2 region of human IgG1 (hMAdCAM-1/Fc) coated surface (10 μg/mL) for 2 h at 37 °C before fixation. For the quantification of cell spreading, outlines of 50 randomly selected adherent cells from each of three separate experiments were generated, and the number of pixels contained within each of these regions was measured by using Image-Pro® plus v6.0.

Wound-Healing Assay. Cells were seeded on h-MAdCAM-1/Fc (10 μg/mL) coated glass coverslips in F12 medium with 0.5% (vol/vol) FBS until cells formed a confluent monolayer. Then the cell monolayer was wounded using a sterile P10 pipette tip. Image sequences were collected at 5 min interval on Leica DM IRE2 microscope with CoolSNAP™ HQ camera (Photometrics).

Single Cell Random Migration. Cells were plated on h-MAdCAM-1/Fc (10 μg/mL) coated glass bottom dish in F12 medium with 0.5% FBS within a CO_2 chamber at 37 °C. After 4 h, image sequences were collected every 5 min. Migration tracks were determined as tracks of cells that did not die, divide, or run out of the field of view during 9 h.

Serum-Induced Transwell Migration. Both sides of transwell chambers (8 μm pore, Millipore) were coated with 10 μg/mL h-MAdCAM-1/Fc. Serum-starved CHO-K1 cells were added to the upper chamber and the lower chamber was filled with F12 medium with 10% FBS. After incubation at 37 °C for 4 h, cells migrating to the lower side were stained with 0.5% Crystal Violet (Sigma) and enumerated by microscopy.

Coimmunoprecipitation. Cells were plated on h-MAdCAM-1/Fc (10 μg/mL) coated surface for 2 h before subjected to immunoprecipitation. Integrins were immunoprecipitated by $\alpha_4\beta_7$ mAb Act-1. Mouse IgG was used as control. Talin, paxillin, and integrin β_7 subunit were detected by antitalin (Sigma-Aldrich), antipaxillin and FIB27 mAbs (BD Biosciences), respectively.

Statistical Analysis. All statistical analysis was performed using a two-tailed Student's t test.

ACKNOWLEDGMENTS. We thank Dr. Minsoo Kim (University of Rochester Medical Center) for kindly providing talin-GFP and Dr. Gaoxiang Ge and Dr. Dangsheng Li for discussion. This work was supported by grants from National Institute of Health (NIH) (HLB-48675), Ministry of Science and Technology 973 project (2010CB529703), National Natural Science Foundation of China (30700119, 30970604), Shanghai Pujiang Program (08PJ14106), Chinese Academy of Sciences (KSCX2-YW-R-67), and Novo Nordisk-CAS Research Foundation (NN-CAS 2008-1).

1. Berlin C, et al. (1993) $\alpha_4\beta_7$ integrin mediates lymphocyte binding to the mucosal vascular addressin MAdCAM-1. *Cell* 74:185–195.
2. Luo B-H, Carman CV, Springer TA (2007) Structural basis of integrin regulation and signaling. *Annu Rev Immunol* 25:619–647.
3. Arnaout MA, Mahalingam B, Xiong JP (2005) Integrin structure, allostery, and bidirectional signaling. *Annu Rev Cell Dev Biol* 21:381–410.
4. Mould AP, Akiyama SK, Humphries MJ (1995) Regulation of integrin $\alpha_5\beta_1$-fibronectin interactions by divalent cations. *J Biol Chem* 270:26270–26277.
5. Leitinger B, McDowall A, Stanley P, Hogg N (2000) The regulation of integrin function by Ca^{2+}. *Biochim Biophys Acta* 1498:91–98.
6. Zhu J, et al. (2008) Structure of a complete integrin ectodomain in a physiologic resting state and activation and deactivation by applied forces. *Mol Cell* 32:849–861.
7. Xiong JP, et al. (2009) Crystal structure of the complete integrin $\alpha_v\beta_3$ ectodomain plus an α/β transmembrane fragment. *J Cell Biol* 186:589–600.
8. Chen JF, Salas A, Springer TA (2003) Bistable regulation of integrin adhesiveness by a bipolar metal ion cluster. *Nat Struct Biol* 10:995–1001.
9. Chen J, Yang W, Kim M, Carman CV, Springer TA (2006) Regulation of outside-in signaling and affinity by the β_2 I domain of integrin $\alpha_L\beta_2$. *Proc Natl Acad Sci USA* 103:13062–13067.
10. Valdramidou D, Humphries MJ, Mould AP (2008) Distinct roles of β_1 metal ion-dependent adhesion site (MIDAS), adjacent to MIDAS (ADMIDAS), and ligand-associated metal-binding site (LIMBS) cation-binding sites in ligand recognition by integrin $\alpha_2\beta_1$. *J Biol Chem* 283:32704–32714.
11. Takagi J, DeBottis DP, Erickson HP, Springer TA (2002) The role of the specificity-determining loop of the integrin β subunit I-like domain in autonomous expression, association with the α subunit, and ligand binding. *Biochemistry* 41:4339–4347.
12. Tsuruta D, et al. (2003) Crucial role of the specificity-determining loop of the integrin β_4 subunit in the binding of cells to laminin-5 and outside-in signal transduction. *J Biol Chem* 278:38707–38714.
13. Takagi J, Kamata T, Meredith J, Puzon-McLaughlin W, Takada Y (1997) Changing ligand specificities of $\alpha_v\beta_1$ and $\alpha_v\beta_3$ integrins by swapping a short diverse sequence of the β subunit. *J Biol Chem* 272:19794–19800.
14. Xie C, et al. (2010) Structure of an integrin with an α I domain, complement receptor type 4. *Embo J* 29:666–679.
15. Springer TA, Zhu J, Xiao T (2008) Structural basis for distinctive recognition of fibrinogen γ C peptide by the platelet integrin $\alpha_{IIb}\beta_3$. *J Cell Biol* 182:791–800.
16. Gallivan JP, Dougherty DA (1999) Cation-π interactions in structural biology. *Proc Natl Acad Sci USA* 96:9459–9464.
17. Mecozzi S, West AP, Jr, Dougherty DA (1996) Cation-π interactions in aromatics of biological and medicinal interest: electrostatic potential surfaces as a useful qualitative guide. *Proc Natl Acad Sci USA* 93:10566–10571.
18. Chen JF, et al. (2004) The relative influence of metal ion binding sites in the I-like domain and the interface with the hybrid domain on rolling and firm adhesion by integrin $\alpha_4\beta_7$. *J Biol Chem* 279:55556–55561.
19. Tidswell M, et al. (1997) Structure-function analysis of the integrin β_7 subunit: identification of domains involved in adhesion to MAdCAM-1. *J Immunol* 159:1497–1505.
20. Kim M, Carman CV, Springer TA (2003) Bidirectional transmembrane signaling by cytoplasmic domain separation in integrins. *Science* 301:1720–1725.
21. Tadokoro S, et al. (2003) Talin binding to integrin β tails: a final common step in integrin activation. *Science* 302:103–106.
22. Fischer W, Franke H, Groger-Arndt H, Illes P (2005) Evidence for the existence of P2Y1,2,4 receptor subtypes in HEK-293 cells: reactivation of P2Y1 receptors after repetitive agonist application. *N-S Arch Ex Path Ph* 371:466–472.
23. Sun DS, et al. (2005) PI3-kinase is essential for ADP-stimulated integrin $\alpha_{IIb}\beta_3$-mediated platelet calcium oscillation, implications for P2Y receptor pathways in integrin $\alpha_{IIb}\beta_3$-initiated signaling cross-talks. *J Biomed Sci* 12:937–948.
24. Butler B, Williams MP, Blystone SD (2003) Ligand-dependent activation of integrin $\alpha_v\beta_3$. *J Biol Chem* 278:5264–5270.
25. Liu S, et al. (1999) Binding of paxillin to α_4 integrins modifies integrin-dependent biological responses. *Nature* 402:676–681.
26. Han J, Rose DM, Woodside DG, Goldfinger LE, Ginsberg MH (2003) Integrin $\alpha_4\beta_1$-dependent T cell migration requires both phosphorylation and dephosphorylation of the α_4 cytoplasmic domain to regulate the reversible binding of paxillin. *J Biol Chem* 278:34845–34853.
27. Huttenlocher A, Ginsberg MH, Horwitz AF (1996) Modulation of cell migration by integrin-mediated cytoskeletal linkages and ligand-binding affinity. *J Cell Biol* 134:1551–1562.
28. Merdek KD, Yang X, Taglienti CA, Shaw LM, Mercurio AM (2007) Intrinsic signaling functions of the β_4 integrin intracellular domain. *J Biol Chem* 282:30322–30330.
29. Xiao T, Takagi J, Wang J-h, Coller BS, Springer TA (2004) Structural basis for allostery in integrins and binding of ligand-mimetic therapeutics to the platelet receptor for fibrinogen. *Nature* 432:59–67.
30. Mould AP, et al. (2003) Conformational changes in the integrin βA domain provide a mechanism for signal transduction via hybrid domain movement. *J Biol Chem* 278:17028–17035.
31. Yang W, Shimaoka M, Chen JF, Springer TA (2004) Activation of integrin β subunit I-like domains by one-turn C-terminal α-helix deletions. *Proc Natl Acad Sci USA* 101:2333–2338.
32. Xiong JP, et al. (2002) Crystal structure of the extracellular segment of integrin $\alpha_v\beta_3$ in complex with an Arg-Gly-Asp ligand. *Science* 296:151–155.
33. Vadlamudi R, Adam L, Tseng B, Costa L, Kumar R (1999) Transcriptional up-regulation of paxillin expression by heregulin in human breast cancer cells. *Cancer Res* 59:2843–2846.
34. Clark EA, Brugge JS (1995) Integrins and signal transduction pathways: the road taken. *Science* 268:233–239.
35. McCubrey JA, et al. (2007) Roles of the Raf/MEK/ERK pathway in cell growth, malignant transformation and drug resistance. *Biochim Biophys Acta* 1773:1263–1284.
36. Scott MJ, Billiar TR (2008) β_2-integrin-induced p38 MAPK activation is a key mediator in the CD14/TLR4/MD2-dependent uptake of lipopolysaccharide by hepatocytes. *J Biol Chem* 283:29433–29446.
37. Armulik A, Velling T, Johansson S (2004) The integrin β_1 subunit transmembrane domain regulates phosphatidylinositol 3-kinase-dependent tyrosine phosphorylation of Crk-associated substrate. *Mol Biol Cell* 15:2558–2567.
38. Lauffenburger DA, Horwitz AF (1996) Cell migration: a physically integrated molecular process. *Cell* 84:359–369.
39. Park EJ, et al. (2007) Aberrant activation of integrin $\alpha_4\beta_7$ suppresses lymphocyte migration to the gut. *J Clin Invest* 117:2526–2538.
40. Goldfinger LE, Han J, Kiosses WB, Howe AK, Ginsberg MH (2003) Spatial restriction of α_4 integrin phosphorylation regulates lamellipodial stability and $\alpha_4\beta_7$-dependent cell migration. *J Cell Biol* 162:731–741.
41. Franco SJ, et al. (2004) Calpain-mediated proteolysis of talin regulates adhesion dynamics. *Nat Cell Biol* 6:977–983.
42. Zhu J, et al. (2007) Requirement of α and β subunit transmembrane helix separation for integrin outside-in signaling. *Blood* 110:2475–2483.